Separation Science and Technology
Publication details, including instructions for authors and subscription information:
http://www.informaworld.com/smpp/title~content=t713708471

Effect of Ion Beam Irradiation on Two Nanofiltration Water Treatment Membranes

Rama Chennamsetty[a]; Isabel Escobar[a]
[a] Department of Chemical & Environmental Engineering, The University of Toledo, Toledo, OH, USA

To cite this Article Chennamsetty, Rama and Escobar, Isabel(2008) 'Effect of Ion Beam Irradiation on Two Nanofiltration Water Treatment Membranes', Separation Science and Technology, 43: 16, 4009 — 4029
To link to this Article: DOI: 10.1080/01496390802414619
URL: http://dx.doi.org/10.1080/01496390802414619

Separation Science and Technology, 43: 4009–4029, 2008

ISSN: 0149-6395 print/1520-5754 online
DOI: 10.1080/01496390802414619

Taylor & Francis
Taylor & Francis Group

Effect of Ion Beam Irradiation on Two Nanofiltration Water Treatment Membranes

Rama Chennamsetty and Isabel Escobar
Department of Chemical & Environmental Engineering,
The University of Toledo, Toledo, OH, USA

Abstract: Ion beam irradiation has long been recognized as an effective method for the synthesis and modification of diverse materials, including polymers. Ion beam irradiation is the bombardment of a substance with energetic ions. When the ions penetrate through the surface of a membrane, they may eliminate tall peaks and deep valleys, resulting in an overall reduction in surface roughness. Two nanofiltration membranes, one with a sulfonated polysulfone selective layer and the other with an aromatic polyamide selective layer, were used to study the effects of ion beam irradiation on surface morphology, microstructure, and performance. A beam of 25 keV H^+ ions with four irradiation fluences (1×10^{13} ions/cm^2, 5×10^{13} ions/cm^2, 1×10^{14} ions/cm^2 and 5×10^{14} ions/cm^2) was used for ion beam irradiation of the membrane. Atomic face microscopy (AFM) analysis show that the roughness of the membranes decreased after irradiation. An increase in flux after ion beam irradiation was also observed. Hydrophobicity, pore size distribution, and selectivity of the membrane were not affected by ion beam irradiation.

Keywords: Ion fluence, irradiation, membrane surface modifications, surface properties, transport properties

INTRODUCTION

Ideal membranes would be able to maintain high throughput of a desired permeate with a high degree of selectivity. Unfortunately, these

Received 16 August 2007; accepted 7 February 2008.
Address correspondence to Isabel Escobar, Department of Chemical & Environmental Engineering, The University of Toledo, 2801 West Bancroft, Nitschke Hall 3048, Toledo, OH 43606, USA. Tel.: +419 530 8267; Fax: 419 530 8086. E-mail: Isabel.escobar@utoledo.edu

two parameters are mutually counteractive. The reason is that a high degree of selectivity is normally only achievable using a membrane having small pores and inherently high hydraulic resistance (or low permeability). Fouling is another severe problem associated with water treatment membranes, which is the deposition of solute constituents onto the surface of the membrane. Fouling of membrane elements often causes a significant increase in hydraulic resistance and applied pressure drop, which increases operating cost and decreases the life of the membrane (1).

Membrane fouling is controlled by the foulant characteristics, feedwater solution chemistry (pH, ionic strength, divalent cation concentration), membrane properties (surface charge, hydrophobicity, roughness), and hydrodynamic conditions (permeate flux, crossflow velocity) (2). In addition to membrane scaling, there are two types of fouling: biofouling and abiotic fouling, which are the focus of this study. Biofouling results from the accumulation of microorganisms on the membrane, while abiotic fouling forms a cake layer consisting of rejected materials, mainly natural organic matter (NOM) on the membrane surface. Since nanofiltration membranes have very small pores, surface fouling which is caused by foulant accumulation (deposition) on the membrane surface is the dominant fouling mechanism in nanofiltration. The severity of abiotic fouling is directly linked to membrane's surface roughness (3). A membrane with high roughness has distinct peaks and valleys. The valleys provide the path of least resistance, therefore a majority of permeate is transported through the membrane via these valleys. However, during operation, the valleys easily become clogged, which initiates membrane fouling and leads to complete blockage of the membrane pores.

For membranes to be competitive with other more established conventional technology, a membrane process needs to operate with a high rate of flux, have a high degree of selectivity and have a high resistance to fouling. Postsynthesis modification involves modifying the membrane after the initial manufacturing process is complete. One such postsynthesis modification is achieved through ion beam irradiation. Ion beam irradiation has long been recognized as an effective method for the synthesis and modification of diverse materials, including polymers (4–6). Ion beam irradiation is the bombardment of a substance with energetic ions. When the ions penetrate through the surface of a membrane, they may eliminate the tall peaks and deep valleys, resulting in an overall reduction in surface roughness (7). As the ions penetrate the membrane, they lose energy to their surroundings (membrane structure) by two main processes: interacting with target nuclei (nuclear stopping) and interacting with target electrons (electronic stopping; (8)). Nuclear stopping

energy losses arise from collisions between energetic particles and target nuclei. Atomic displacement occurs when the colliding ion imparts energy greater than certain displacement threshold energy. If the energy is not great enough for displacement, the energy dissipates as atomic vibrations known as phonons. The threshold energy is the energy that a recoil requires to overcome binding forces and to move more than one atomic spacing away from its original site. The interaction of an ion with a target nucleus is treated as the scattering of two screened particles since the nuclear collision occurs between two atoms with electrons around protons and neutrons. Nuclear stopping varies with ion velocity as well as the charges of two colliding atoms, as it is derived with consideration of the momentum transfer from ion to target atom and the interatomic potential between two atoms.

Electronic stopping energy losses arise from electromagnetic interaction between the positively charged ions and the target electrons. There are two mechanisms: one is called glancing collision (inelastic scattering, distant resonant collisions with small momentum transfer), which is quite frequent but each collision involves a small energy loss (<100 eV). The other is called knock-on collision (elastic scattering, close collisions with large momentum transfer), which is very infrequent but each collision imparts a large energy to a target electron (>100 eV). Both collisions transfer energy in two ways: electronic excitation and ionization. Excitation is the process in which an electron jumps to a higher energy level, while in ionization an orbital electron is ejected from the atom.

There have been a number of studies examining the effects of ion beam irradiation on gas separation membranes (7,9–11). These studies exposed polyimide gas separation membranes to different ion irradiation fluences and energies. Ion irradiation fluences refer to the number of ions implanted into a unit of area of the membrane. Ion energy is directly related to the depth the ions and will penetrate into the membrane. As discussed earlier, ion beam irradiation provides energy to the electrons and nuclei of the membrane. The intensive energy deposition in polymers can lead to the following:

1. formation of volatile molecules and free radicals which leave defects in the polymer matrix,
2. creation of additional crosslinking between polymer chains,
3. formation of new chemical bonds, and
4. chemical reactions with chemical atmosphere such as oxidation (10).

These four events can, in turn, lead to membrane microstructure alterations. Previous studies (9–11) found ion beam irradiation resulted in gas separation membranes with both increased permeability and

selectivity; two characteristics which have a trade-off relationship toward each other. The improvements in membrane performance were believed to be results of microstructure modification, which was proven by a narrow but intensive free volume distribution. Studies of atomic force microscopy (AFM) of ion beam irradiated polyimide films showed that ion beam irradiation eliminates deep valleys and tall peaks on the surface of the polyimide films even at very low doses of irradiation and that a very smooth surface can be observed after ion beam irradiation (5).

The goal of the study described here was to determine the effects of ion beam irradiation on surface morphology, microstructure, chemical structure, and also changes in the performance of a modified commercial sulfonated polysulfone and polyamide nanofiltration water treatment membranes.

EXPERIMENTAL

Membrane Properties

Two nanofiltration membranes, one with a sulfonated polysulfone selective layer and the other with an aromatic polyamide selective layer, were used to study the effects of ion beam irradiation on surface morphology, microstructure, and performance.

Polysulfone Membrane

The polysulfone membrane is a commercially available nanofiltration composite membrane with a selective layer of sulfonated polysulfone (NTR 7450, Hydranautics, San Diego, CA). The structure of the sulfonated polysulfone is shown in Fig. 1. The membrane is negatively charged (at pH = 7.0, the charge is −6.26 mV), hydrophobic (contact angle of 58°; ((12), and Table 1) and has a molecular weight cutoff (MWCO) of 1000 Da (13). The operating temperature range is 0–45°C and the pH range is 2–11, and the membrane is able to withstand chlorine concentrations of several hundred ppm.

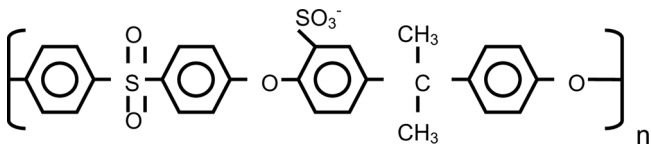

Figure 1. Structure of sulfonated polysulfone.

Table 1. Contact angle measurements of virgin and irradiated membranes

	Contact angle	
Membrane type	Polysulfone	Polyamide
Virgin	59° (±6°)	49° (±4°)
1×10^{13} ions/cm^2	58° (±2°)	46° (±4°)
5×10^{13} ions/cm^2	60° (±2°)	47° (±5°)
1×10^{14} ions/cm^2	59° (±3°)	52° (±4°)
5×10^{14} ions/cm^2	59° (±3°)	46° (±5°)

Polyamide Membrane

The polyamide membrane is also a commercially available nanofiltration composite membrane, and it consists of a polysulfone support layer covered by aromatic polyamide selective layer (TFC-S, Koch Membranes, San Diego, CA). The structure of the polyamide is shown in Fig. 2. Its functional groups are carboxylate/carboxylic acid. The film layer is approximately 1,000–2,000 angstroms thick and the molecular weight cutoff is around 200–300 Da (14,15). The membrane has a slight negative charge with a contact angle of 55° ((16), and Table 1). The typical operating pressure is 80 psi, with the maximum operating pressure being 350 psi. The maximum operating temperature is 45°C and the allowable pH range is 4–11. Chlorine tolerance is low, with the maximum continuous free chlorine concentration being <0.1 mg/l.

Ion Beam Irradiation

Each membrane was irradiated with H^+ ions at an energy level of 25 keV. The incident energy of 25 keV was determined using a well-known

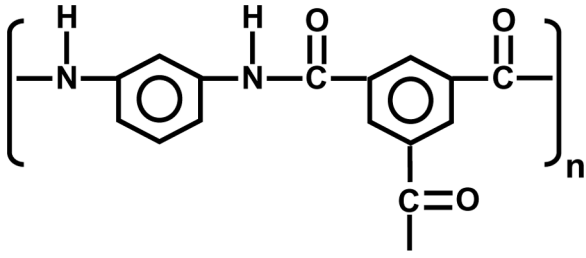

Figure 2. Structure of polyamide.

program titled "The Stopping and Range of Ions in Matter" (SRIM; (17) to ensure that the entire upper semipermeable sulfonated polysulfone layer was modified. When an energetic ion penetrates a polymer, it undergoes a series of collisions with the atoms and electrons in the target matrix. In these collisions, the implanted ion loses its energy by means of both the nuclear and the electronic interactions with the polymer, depending on the energy, atomic number of the ion as well as the polymer material. The nuclear interactions consist of individual elastic collisions between the ion and target atom nuclei, whereas the electronic interactions can be viewed more as a continuous viscous drag phenomenon between the injected ion and the sea of electrons surrounding the target nuclei. The passage of an energetic ion in a polymer is illustrated in Fig. 3. As shown in this figure, the ion does not travel in a straight path to its resting place due to collisions with target atoms. The range, R, is the total distance that the ion travels before coming to rest. However, in many applications of energetic ions in surface modification, it is not the total distance R traveled by the ion that is of interest but the projection of R normal to the surface (i.e. the penetration depth or the projected range R_P). The mean projected range (R_P), increases with ion energy and decreases with atomic number of the ion. The main parameters governing the penetration depth are the energy and atomic number of the implanted ion.

The composite membrane was characterized by a thin semipermeable selective layer (2000 Å to 4000 Å thick), supported on a porous substrate (about ~50 μm thick) that, in turn, is bonded to a fibrous layer, which provides mechanical strength to the top layers without adding significant

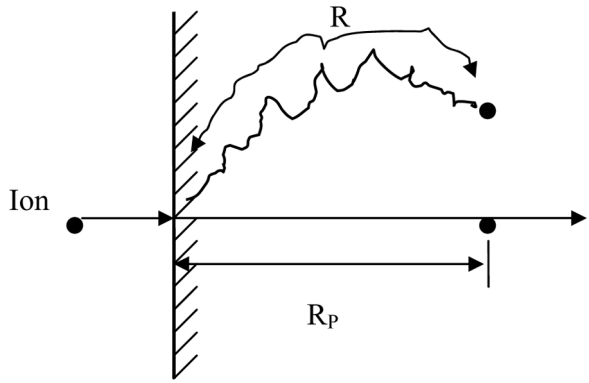

Figure 3. The passage of an energetic ion in a polymer during ion beam irradiation with a total ion path length R, which gives a projected range, R_P, along the direction parallel to that of the incident ion.

hydrodynamic resistance. Figure 4 shows the projectile ranges for the polysulfone and polyamide membranes for different incident energies. The projected ranges and also the electronic and nuclear stopping energy losses were determined using a well-known program titled "The Stopping and Range of Ions in Matter" (SRIM) to ensure that the entire upper semipermeable selective layer was modified. From the projectile ranges in Fig. 4, incident energy of 25 keV was chosen to ensure that the entire upper semipermeable selective layer was modified by the ion beam irradiation for both the polysulfone and polyamide membranes.

Four irradiation fluences (1×10^{13} ions/cm^2, 5×10^{13} ions/cm^2, 1×10^{14} ions/cm^2 and 5×10^{14} ions/cm^2) were used for ion beam irradiation of the membranes. The beam current density was maintained at low levels ($<1\,\mu$A/cm^2) to avoid heating of the samples. All samples were irradiated at room temperature and in a vacuum chamber at a pressure less then 1.9×10^{-7} torr. The incident beam was perpendicular to the samples. The ion beam irradiation used here was not sputtering off the membrane with ions, so the incident angle would not lead to a significant decrease in roughness. The method used is the implantation of the H^+ ion into the surface of the membrane. The decrease of roughness after irradiation is not a function of just blasting off the peaks with ions; instead, irradiation resulted in local heating of the samples and in crosslinking, which resulted in the roughness decrease. The irradiation was performed

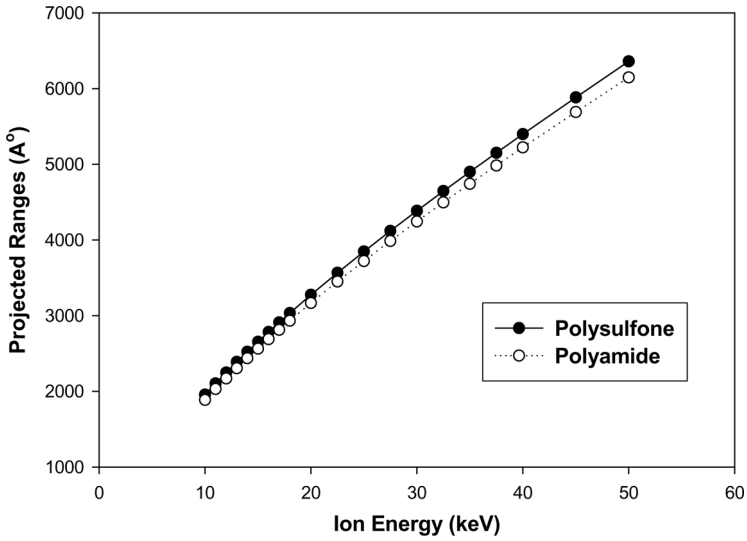

Figure 4. Projectile ranges of the H^+ ions in the polysulfone and polyamide membranes with various ion energies.

using a 1.7 MV high current Tandetron Accelerator at the University of Michigan (Ann Arbor, Michigan). To provide support to the membrane through the irradiation process, a foil tape masking was utilized. Only the active area of the membrane, which was about a circular area of 95 cm^2, was irradiated.

Contact Angle Analysis

The contact angle measurements were performed using distilled water on the top surface of the membranes using Cam-Plus Micro contact angle meter (Tantec Inc., Schaumburg, IL). Sessile Drop, Half-Angle^{TM} measuring method (U.S. Patent No. 5,268,733) was used for measuring the contact angles. The measurements were performed at room temperature.

Pore Size Distribution Analysis

The pore size distribution analyses were performed using polyethylene glycol (PEG) of various molecular weights (ranging from 200 g/mol to 4600 g/mol). For the polysulfone membrane, (molecular weight cutoff of 1000 Da), the pore size distribution analyses were conducted by using various molecular weights of PEG ranging from 200 g/mol to 4600 g/mol, while for polyamide, (molecular weight cutoff of around 200–300 Da), the pore size distribution analyses were conducted by using various molecular weights of PEG ranging from 200 g/mol to 1000 g/mol.

Atomic Force Microscope (AFM) Analysis

Atomic force microscopy (AFM) was used for evolution in surface morphology. AFM allows acquiring 3D topographic data with a high vertical resolution. Accurate and quantitative data about surface morphology are provided over a wide range of magnifications and can be used in several quantitative analyses approaches such as the section, bearing, and roughness analysis. AFM measurements were performed using a Nanoscope IIIa Scanning Probe Microscopy (Digital Instruments, Santa Barbara, CA).

Bench-Scale Cross-Flow

The membrane was housed in a SEPA CF cross-flow filtration unit (Osmonics, Minneatonka, MN). The filtration unit was constructed out

of 316 stainless steel and rated for an operating pressure up to 69 bar (1000 psi). The test unit was sealed by applying adequate pressure via a hand pump (P-142, Enerpac, Milwaukee, WI) which actuated a piston on the SEPA CF, sealing the membrane within the membrane cell. The feed stream was delivered by a motor (Baldor Electric Company, Ft. Smith, AR and Dayton Electric Manufacturing Co., Niles, IL) and M-03 Hydra-cell pump (Wanner Engineering, Inc., Minneapolis, MN) assembly. Flow valves controlled permeate and retenate (also called concentrate) flow and the pressure acting on the membrane in the test unit. Due to the high pressures required by the membranes, it was necessary to control the temperature of the feed water using a chiller (Model KR60A, Cole-Parmer Instrument Company, Veenon Hills, Illinois) to keep it at approximately 20°C. The schematic diagram of the filtration assembly is shown in Fig. 5.

The SEPA CF unit required a membrane area of 139 cm^2, but membrane size was restricted to a circular area of 95 cm^2 because of limitations of the chosen irradiation method. The required area was reduced to accommodate the sample size by applying a foil tape masking around the membrane (necessary also for irradiation purposes).

The membranes were tested with raw water containing bovine serum albumin protein with a concentration of 10 mg/L and 1 mmole/L of $CaCl_2$. Before testing began, each membrane was thoroughly rinsed with deionized (DI) water and soaked in DI water overnight (18). The membrane was removed from the DI water and thoroughly rinsed with DI water again immediately before placing the membrane into the filtration

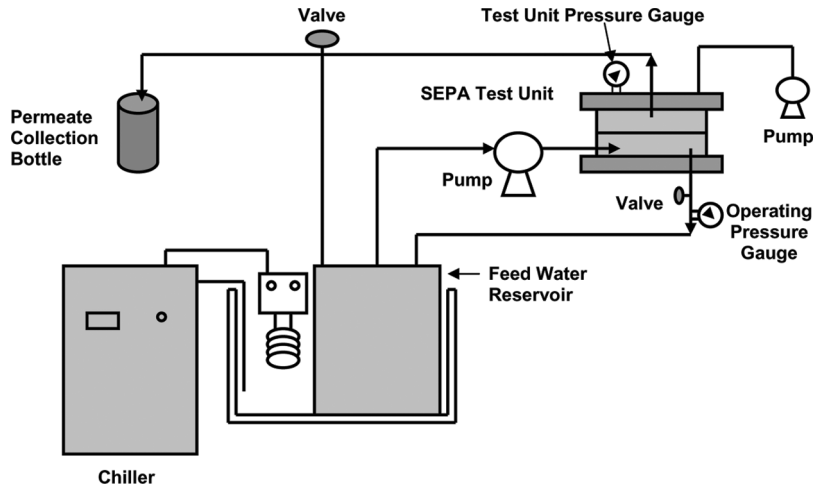

Figure 5. Schematic diagram showing the filtration assembly.

cell unit. After installation, the membrane was pre-compacted by filtering 250 mL of DI water. The pre-soaking and initial DI water flush were required to stabilize the flux and rejection of the membrane. Initially, membrane pores were filled with air; soaking and pre-compaction forces out these air bubbles, allowing a "steady-state" operation of the membrane prior to filtration of raw water. The synthetic raw water was added to the feed reservoir and permeate samples were collected at regular intervals of time.

The selectivity analyses were performed by measuring the rejections using monovalent cations (NaCl – 10 mmol/L), divalent cations ($CaCl_2$ – 10 mmol/L) and by using Orange II dye (molecular weight of 350 g/mol) with a concentration of 10 mg/L. The concentrations of the salts were analyzed by traceable expanded range digital conductivity meter (Fischer Scientific) and the orange II dye was analyzed by using UV Spectrophotometer (UV-2401 PC, Shimadzu Scientific Instruments, Addison, IL) at 486 nm wavelength.

RESULTS AND DISCUSSION

The sulfonated polysulfone membranes were bombarded at ion fluences in the following ranges:

1. small fluence at 1×10^{13} H^+ ions/cm^2,
2. intermediate fluences at 5×10^{13} H^+ ions/cm^2 and 1×10^{14} H^+ ions/cm^2, and
3. high fluence at 5×10^{14} H^+ ions/cm^2.

The color of the virgin membrane was white and changed to light brown after ion beam irradiation with an ion fluence of 1×10^{13} H^+ ions/cm^2. The intensity of the color increased as the irradiation dose was increased from ion fluence 1×10^{13} H^+ ions/cm^2 to 5×10^{14} H^+ ions/cm^2.

In order to determine the effects of ion beam irradiation on the chemical structure of the membrane, ATR/FTIR analysis was performed on the irradiated membranes and was compared with the ATR/FTIR analysis of the virgin membrane. FTIR spectra of the virgin and irradiated polysulfone membranes have shown increase in the peak heights at 690 cm^{-1} wavenumber and decrease in peak heights at 920 cm^{-1} and 1041 cm^{-1} wavenumbers, which correspond to the C–S–C bond, C–H bond out of plane vibrations and SO_3 bond, respectively (19). Ion beam irradiation resulted in breaking of SO_3 and C–H bonds along with the formation of C–S–C bonds. These are hypothesized to have led to an increase in cross linking. For the polyamide membranes, ion beam

irradiation resulted in decrease in the peak heights at 1080 cm^{-1} and 1320 cm^{-1} wavenumbers, which correspond to the CO–NH bond and C–H bond, respectively. Therefore, ion beam irradiation resulted in breaking some of CO–NH and C–H bonds in the polyamide membrane.

Figures 6 and 7 show the AFM images of the virgin and irradiated membranes for the polysulfone and polyamide membranes, respectively. The area of the image is 5×5 μm in the xy-plane with an expanded z-axis of 5 nm for the polysulfone membrane and with an expanded z-axis of 50 nm for the polyamide membrane. The intensity of the shading in the AFM images indicates the vertical profile of the membrane surface with the light regions being the highest points and the dark regions being depressions. It should be emphasized that all micrographs are representative pictures of membrane surface as no difference can be observed from these images for various parts of the membrane surface. The images were reproducible in different directions and spots. Nodular structures were observed at the top surface for both the polysulfone and polyamide membranes. Nodules structures at the top surface for flat sheet membranes were also found in earlier studies (20–22).

The average roughness of the virgin sulfonated polysulfone membrane was 5.63 nm ($\pm$ 1.32 nm) and that of polyamide membrane was 36.6 nm ($\pm$ 4.2 nm). There have been a number of studies (3,23–25) examining the close relationship between membrane surface characteristics and fouling with a conclusion that fouling might be minimized using a membrane with lower surface roughness. The nodular structures for the polyamide membranes are more distinct and are clearly observed when compared to the polysulfone membrane, which has a very smooth

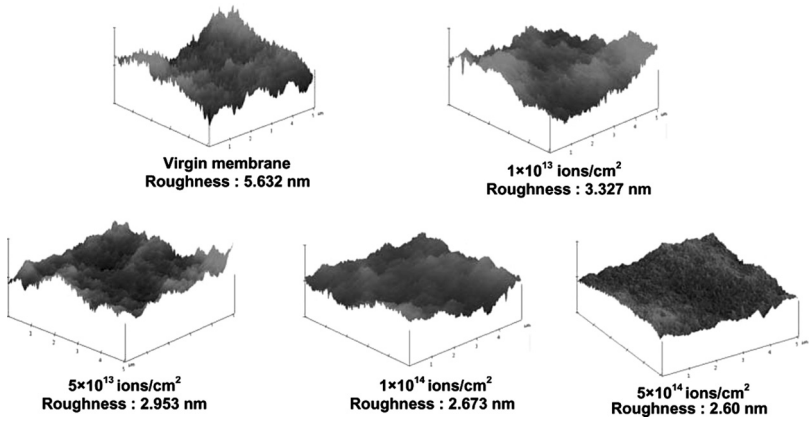

Figure 6. AFM images of the polysulfone membranes.

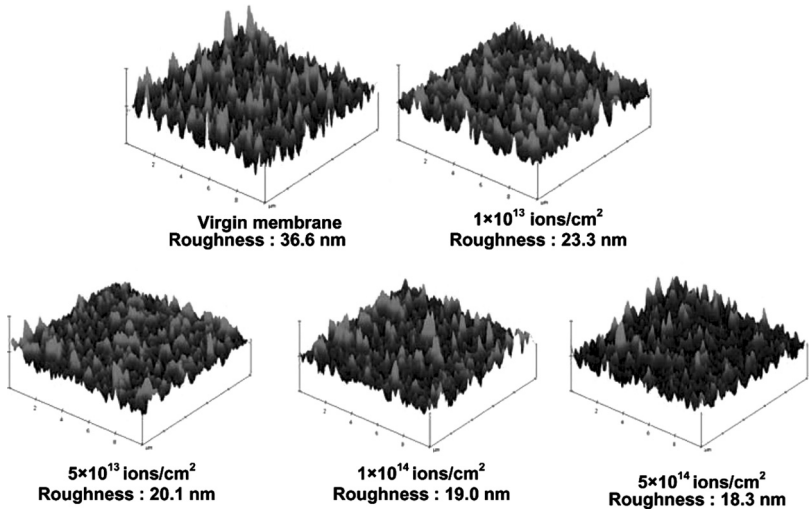

Figure 7. AFM images of the polyamide membranes.

surface. During operation of the membranes the valleys between the nodular-like structures for the polyamide membrane can be easily become clogged when compared to the polysulfone membrane. The clogging initiates the membrane fouling and leads to complete blockage of the membrane pores.

The average roughness of the polysulfone membrane was decreased to 3.33 nm ($\pm$ 0.73 nm) after irradiation of the membrane with an ion fluence of 1×10^{13} ions/cm^2. The roughness of the irradiated membranes with ion fluences of 5×10^{13} ions/cm^2, 1×10^{14} ions/cm^2 and 5×10^{14} ions/cm^2 were 2.95 nm ($\pm$ 0.89 nm), 2.67 nm ($\pm$ 0.63 nm) and 2.60 nm ($\pm$ 0.70 nm), respectively. The average decreases in roughness were 41%, 48%, 53%, and 54% after irradiation with ion fluences of 1×10^{13} ions/cm^2, 5×10^{13} ions/cm^2, 1×10^{14} ions/cm^2, and 5×10^{14} ions/cm^2, respectively, from the virgin polysulfone membrane. These were all statistically different from the virgin membrane roughness values (all p-values were less than 0.0001). The trend of decrease in roughness with ion fluence is shown in Fig. 8.

The average roughness of the polyamide membrane was decreased to 23.3 nm ($\pm$ 2.6 nm) after irradiation of the membrane with an ion fluence of 1×10^{13} ions/cm^2. The roughness of the irradiated membranes with ion fluences of 5×10^{13} ions/cm^2, 1×10^{14} ions/cm^2 and 5×10^{14} ions/cm^2 were 20.1 nm ($\pm$ 1.8 nm), 19.0 nm ($\pm$ 2.4 nm) and 18.3 nm ($\pm$ 1.9 nm), respectively. The average decreases in roughness were 36%, 45%, 48%,

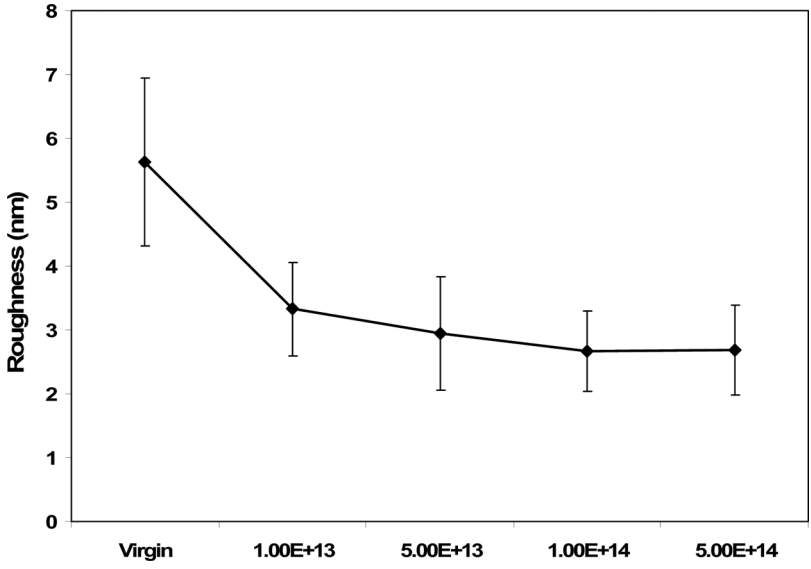

Figure 8. Roughness and % reduction of the virgin and the irradiated polysulfone membranes.

and 50% after irradiation with ion fluences of 1×10^{13} ions/cm^2, 5×10^{13} ions/cm^2, 1×10^{14} ions/cm^2, and 5×10^{14} ions/cm^2, respectively, from the virgin polyamide membrane. These were all statistically different from the virgin membrane roughness values (all p-values were less than 0.0001). The trend of decrease in roughness with ion fluence is shown in Fig. 9.

For both the membranes there was a slight decrease in the roughness from the virgin membranes. AFM analyses indicate that nodule-like structures of the unmodified membrane were smoothened after ion beam irradiation. This decrease was expected as observed with gas separation membranes (5). The changes in nodular structures were more clearly observed for the polyamide membrane which has higher roughness then the polysulfone membrane.

The observed contact angles for the virgin polysulfone and polyamide membrane were approximately 59° and 49°, respectively (Table 1), which were consistent with values reported in the literature (12,16). The contact angles for the irradiated membranes at different ion fluences for both the polysulfone and poyamide membranes were not different from the virgin polysulfone and poyamide membranes, which confirmed that the hydrophobic character of the membrane was not changed after ion beam irradiation.

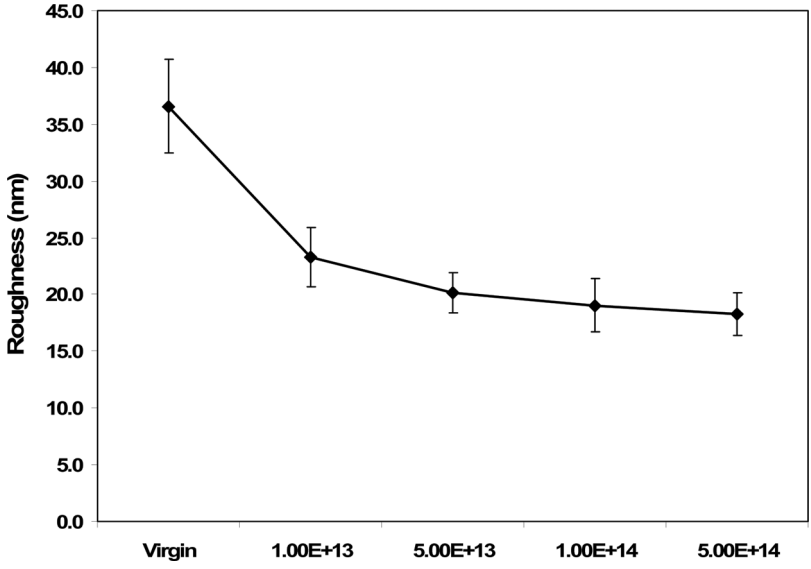

Figure 9. Roughness and % reduction of the virgin and the irradiated polyamide membranes.

Figures 10 and 11 represent the pore size distribution analyses of the virgin and irradiated membranes for the polysulfone and polyamide membranes respectively which show the changes in the solute rejections of model compounds with varying diameters. The analyses show that the pore size distribution was not affected by the ion beam irradiation for both the membranes. Since the hydrophobic character and pore size distribution were not changed after ion beam radiation, the rejection values should not change after ion beam irradiation which was confirmed by comparing the rejection values of both virgin and irradiated membranes. The pore size distribution analysis were done using polyethylene glycol molecules which were not charged when compared to the rejection analysis shown in Table 2 where the feed particles are charged. The rejection of the polyethylene glycol depends only on the pore size of the membranes; thus, it shows whether there were any changes in pore size distribution after irradiation. The rejection of the charged particles depends both on the pore size and charge of the membranes.

Table 2 shows the rejection values for the virgin and irradiated polysulfone membranes. The rejections of monovalent cations (NaCl) and divalent cations ($CaCl_2$) were 35% and 64%, respectively, for the virgin polysulfone membrane. The rejection values for both salts were not changed after ion beam irradiation at different ion fluences for the polysulfone

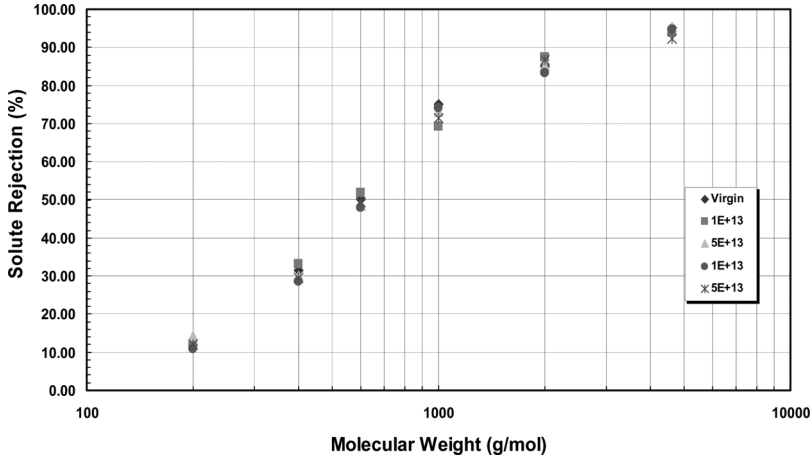

Figure 10. Pore size distribution analysis of virgin and irradiated polysulfone membranes.

membrane. Due to a limited number of irradiated membrane samples replication was not performed to all rejection experiments. Therefore, standard deviations are not shown. The rejection of the orange II dye was about 92% for the virgin polysulfone membrane and decrease slightly to 89% after irradiation of the membrane with an ion fluence of 1×10^{13} ions/cm^2. The rejection values of the irradiated membranes with ion fluences of 5×10^{13} ions/cm^2, 1×10^{14} ions/cm^2 and 5×10^{14} ions/cm^2 were 86%, 88%, and 86%, respectively. The slight decrease in the rejection

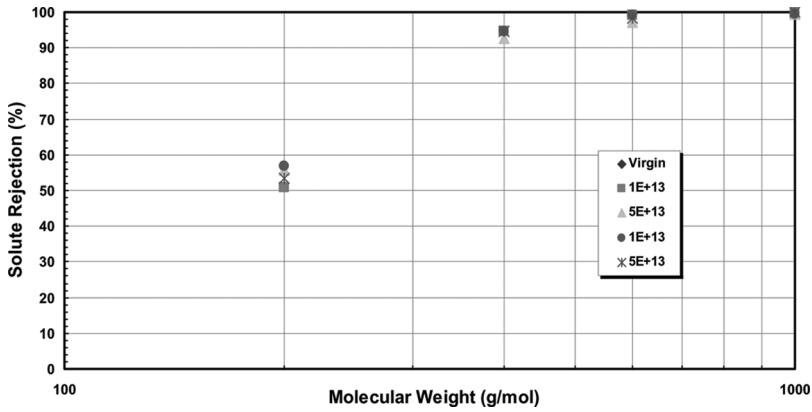

Figure 11. Pore size distribution analysis of virgin and irradiated polyamide membranes.

Table 2. % of Rejections of the polysulfone membrane

Solute	Virgin	1×10^{13} ions/cm^2	5×10^{13} ions/cm^2	1×10^{14} ions/cm^2	5×10^{14} ions/cm^2
NaCl	35	33	36	31	33
$CaCl_2$	64	62	63	62	61
Orange II (MW 350)	92	89	86	88	86

values for the orange II dye can be expected from the decrease in the fouling of the membrane after irradiation. The cake layer, which is the fouling on the membrane, provides an additional porous surface through which the liquid must pass and as a result the cake layer increases the particle removal efficiency of the membrane. As the cake layer was decreased after irradiation, a slight decrease in rejection of the orange II dye resulted. Table 3 shows the rejection values for the virgin and irradiated polyamide membranes. The rejections of monovalent cations (NaCl) and divalent cations ($CaCl_2$) were 84% and 96%, respectively, for the virgin polyamide membrane and were not changed after irradiation of the membrane. 100% rejection was observed for orange II dye as the molecular weight of the polyamide membrane is smaller. There was no change in the rejection values of the orange II dye after irradiation of the polyamide membrane. The rejection analyses show that the separation capabilities of the membrane were not affected by ion beam irradiation for both the membranes.

Figures 12 and 13 represent the flux analyses for the virgin and irradiated membranes for the polysulfone and polyamide respectively, which were run with feed water containing protein and $CaCl_2$. Normalized fluxes were defined as the ratio of the irradiated membrane flux to the virgin membrane flux at the start of filtration. The flux was normalized to compare the change in flux decline of the membrane after irradiation. The analyses show that the flux was increased after ion beam irradiation. The increase in the flux values for the four irradiated polysulfone

Table 3. % of Rejections of the polyamide membrane

Solute	Virgin	1×10^{13} ions/cm^2	5×10^{13} ions/cm^2	1×10^{14} ions/cm^2	5×10^{14} ions/cm^2
NaCl	84	82	84	81	81
$CaCl_2$	96	95	93	95	94
Orange II (MW 350)	100	100	100	100	100

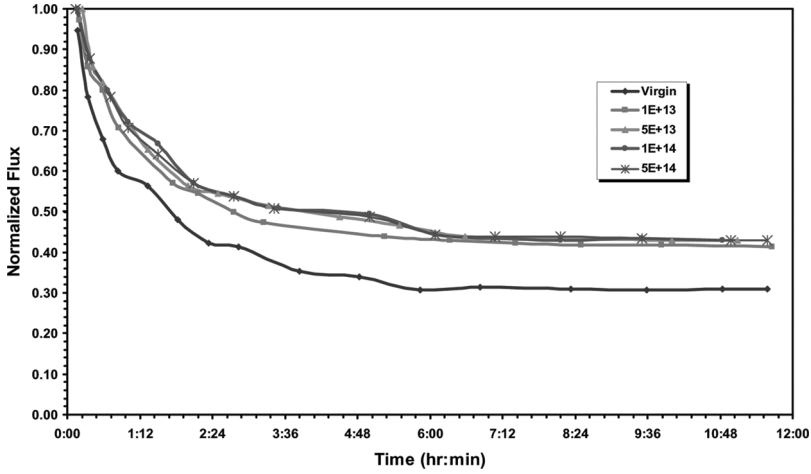

Figure 12. Flux vs time of virgin and irradiated polysulfone membranes.

membranes with ion fluences 1×10^{13} ions/cm^2, 5×10^{13} ions/cm^2, 1×10^{14} ions/cm^2 and 1×10^{14} ions/cm^2 were 33%, 38%, 40% and 40%, respectively, after 10 hrs of operation. The increase in the flux values for the four irradiated polyamide membranes with ion fluences 1×10^{13} ions/cm^2, 5×10^{13} ions/cm^2, 1×10^{14} ions/cm^2 and 1×10^{14} ions/cm^2 were 57%, 61%, 65%, and 64%, respectively, after 10 hrs of operation.

Under the experimental conditions used, the decrease in roughness after irradiation was not enough to lead to a thinning of the membrane.

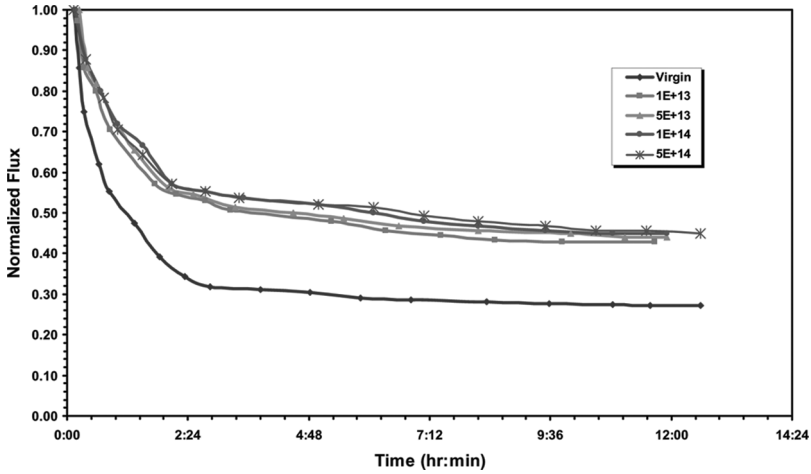

Figure 13. Flux vs. time of virgin and irradiated polyamide membranes.

As there was no significant change in either membrane thickness or membrane hydrophobicity, there was no change in membrane pure water flux after irradiation (data not shown here). Surface roughness is an important characteristic of the membrane, which influences the rate and extent of fouling (15,16). A membrane that exhibits high roughness inherently has distinct peaks and valleys. The valleys provide paths of least resistance, therefore a majority of permeate is transported through the membrane via these valleys. However, during operation, the valleys easily become clogged, which initiates membrane fouling and leads to flux decline and eventually complete blockage of the membrane pores. Therefore, the decrease in roughness of the membrane after ion beam irradiation resulted in a decrease in fouling, as measured by a decrease in flux decline during operations, of the membrane.

CONCLUSIONS

The major impacts of ion beam irradiation as a post-synthesis modification technique were:

- The effect of ion beam irradiation was similar for both the polysulfone and polyamide membranes.
- Ion beam irradiation resulted in rearrangement of atoms in the membrane, microstructure alterations of the surface layer, and decrease in roughness.
- The magnitude of the effect of ion beam irradiation on decrease in roughness increased with increase in ion fluence.
- The hydrophobicity and the pore size distribution of the membranes were not affected by ion beam irradiation.
- Ion beam irradiation resulted in an increase in flux without changing the selectivity.
- As the effect of ion beam irradiation is a decrease in membrane roughness, improvements in operational properties of the polyamide membranes were higher then of the polysulfone membranes as the former have higher roughness then the latter.

Therefore, as the time taken to irradiate at low ion fluences is smaller than at high ion fluences and irradiation time is proportional to irradiation costs, it is deemed better to operate at low ion fluences. Many studies have focused on decreasing membrane flux decline by making membrane more hydrophilic. The work presented here shows that decreasing membrane surface roughness, while keeping membrane hydrophobicity nearly constant, is an effective method of decreasing flux

decline without any losses in rejection efficiency. Therefore, low ion fluence, or less expensive ion beam irradiation, is a method of improving membrane performance as measured by a decrease in flux decline.

ACKNOWLEDGMENTS

This project was funded by the National Science Foundation grant CTS 03-31778. The authors acknowledge Dr. Peter Simpson (University of Western Ontario) and the Michigan Ion Beam Laboratory (University of Michigan) where irradiation was performed and Dr. Mark Wilf provided the membrane samples.

REFERENCES

1. Escobar, I.C.; Hoek, E.M.; Gabelich, C.J.; DiGiano, F.A.; Le Gouellec, Y.A.; Berube, P.; Howe, K.J.; Allen, J.; Atai, K.Z.; Benjamin, M.M.; Brandhuber, P.J.; Brant, J.; Chang, Y.J.; Chapman, M.; Childress, A.; Conlon, WJ.; Cooke, T.H.; Crossley, I.A.; Crozes, G.F.; Huck, P.M.; Kommineni, S.N.; Jacangelo, J.G.; Kaeimi, A.A.; Kim, J.H.; Lawler, D.F.; Li, Q.L.; Schiddeman, L.C.; Sethi, S.; Tobiason, J.E.; Tseng, T.; Veerapanemi, S.; Zander, A.K. (2005) Recent advances and research needs in membrane fouling. *Journal American Water Works Association*, *97*: 79–89.
2. Qilin, Li.; Elimelech, M. (2004) Organic fouling and chemical cleaning of nanofiltration membranes: Measurements and mechanisms. *Environmental Science & Technology*, *38*: 4683–4693
3. Vrijenhoek, E.M.; Hong, S.; Elimelech, M. (2001) Influence of membrane surface properties on initial rate of colloidal fouling of reverse osmosis and nanofiltration membranes. *Journal of Membrane Science*, *188*: 115–128.
4. Davenas, J.; Xu, X.L.; Boiteux, G.; Sage, D. (1989) Relation between structure and electronic properties of ion irradiation polymers. *Ncl. Instr. and Meths in Phys. Res*, *8&9*: 754–763.
5. Xu, X.L.; Dolveck, J.Y.; Boiteux, G.; Escoubes, M.; Monchanin, M.; Dupin, J.P.; Davenas, J. (1995a) A new approach to microporous materials – application of ion beam technology to polyimide membranes. *Mat. Res. Soc. Symp. Proc.*, *354*: 351–356.
6. Xu, X.L.; Dolveck, J.Y.; Boiteux, G.; Escoubes, M.; Monchanin, M.; Dupin, J.P.; Davenas, J. (1995b) Ion beam irradiation effect on gas permeation properties of polyimid films. *Journal of Applied Polymer Science*, *55*: 99–107.
7. Xu, X.L.; Coleman, M.R. (1997) Atomic force microscopy images of ion-implanted 6FDA-pMDA polyimide films. *Journal of Applied Polymer Science*, *66*: 459–469.
8. Lee, E.H. (1999) Ion-beam modification of polymeric materials: Fundamental principles and applications. *Nuclear Instruments and Methods in Physics Research B*, *151*: 29–41.

9. Xu, X.; Coleman, M.R. (1999a) Ion beam irradiation: An efficient method to modify the sub-nanometer scale microstructure of polymers in a controlled way. *Mat. Res.Soc. Symp. Proc.*, *540*: 255–260.
10. Xu, X.; Coleman, M.R. (1999b) Preliminary investigation of gas transport mechanism in a H^+ irradiated polyamide-ceramic composite membrane. *Nuclear Instruments and methods in Physics Research b.*, *152*: 325–334.
11. Xu, X.L.; Coleman, M.R.; Myler, U.; Simpson, P.J. (2000) Post-synthesis method for development of membranes using ion beam irradiation of polyimide thin films. In: *Membrane Formation and Modification*, Pinnau, I.; Freeman, B.D., eds.; Oxford University Press: Washington, D.C., 205–227.
12. Mänttäri, M.; Puro, L.; Nuortila-Jokinen, J.; Nyström, M. (2000) Fouling effect of polysaccharides and humic acid in nanofiltration. *Journal of Membrane Science*, *165*: 1–17.
13. Bargeman, G.; Vollenbroek, J.M.; Straatsma, J.; Schroën, C.G.P.H.; Boom, R.M. (2005) Nanofiltration of multi-component feeds. Interactions between neutral and charged components and their effect on retention. *Journal of Membrane Science*, *247*: 11–20.
14. Koyuncu, I. (2003) An advanced treatment of high-strength opium alkaloid processing industry wastewaters with membrane technology: Pretreatment, fouling and retention characteristics of membranes. *Desalination*, *155*: 265–275.
15. Liikanen, R.; Miettinen, I.; Laukkanen, R. (2003) Selection of NF membrane to improve quality of chemically treated surface water. *Water Research*, *37*: 864–872.
16. Norberg, D.; Hong, S.; Taylor, J.; Zhao, Y. (2002) Surface characterization and performance evaluation of commercial fouling resistant low-pressure RO membranes. *Desalination*, *202*: 45–52.
17. Ziegler, J.F.; Biersack, J.P.; Littmark, U. (Eds.) (1985) *The Stopping and Range of Ions in Solids*, Volume 1. Pergamon Press: New York.
18. Hong, S.; Elimelech, M. (1997) Chemical and physical aspects of natural organic carbon (NOM) fouling of nanofiltration membranes. *Journal of Membrane Science*, *132*: 159–181.
19. Chennamsetty, R.; Escobar, I.; Xu, X. (2006) Polymer evolution of a sulfonated polysulfone membrane as a function of ion beam irradiation fluence. *Journal of Membrane Science*, *280*: 253–260.
20. Kim, J.Y.; Lee, H.K.; Kim, S.C. (1999) Surface structure and phase separation mechanism of polysulfone membranes by atomic force microscopy. *Journal of Membrane Science*, *163*: 159.
21. Dietz, P.; Hansma, P.K.; Inacker, O.; Lehmann, H.-D.; Herrmann, K.-H. (1992) Surface pore structures of micro- and ultrafiltration membranes imaged with the atomic force microscope. *Journal of Membrane Science*, *65*: 101.
22. Fritzsche, A.K.; Arevalo, A.R.; Moore, M.D.; Elings, V.B.; Kjoller, K.; Wu, C.M. (1992) The surface structure and morphology of polyvinylidene fluoride microfiltration membranes by atomic force microscopy. *Journal of Membrane Science*, *68*: 65.

23. Chung, T.-S.; Qin, J.-J.; Huan, A.; Toh, K.-C. (2002) Visualization of the effect of die shear rate on the outer surface morphology of ultrafiltration membranes by AFM. *Journal of Membrane Science*, *196*: 251–266.
24. Madaeni, S.S. (2004) Effect of surface roughness on retention of reverse osmosis membranes. *Journal of Porous Materials*, *11*: 255–263.
25. Bowen, W.R.; Doneva, T.A. (2000) Atomic force microscopy studies of membranes: Effect of surface roughness on double-layer interactions and particle adhesion. *Journal of Colloid and Interface Science*, *229*: 544.